Water Science and Engineering 2022, 15(2): 141−151

HOSTED BY

ELSEVIER

Available online at www.sciencedirect.com

Water Science and Engineering

journal homepage: wse.hhu.edu.cn

Groundwater discharge drives water quality and greenhouse gas emissions in a tidal wetland

Zhi-lin Wang, Mahmood Sadat-Noori*, William Glamore

Water Research Laboratory, School of Civil & Environmental Engineering, University of New South Wales Sydney, Sydney, NSW 2052, Australia

Received 10 December 2021; accepted 5 February 2022
Available online 31 March 2022

Abstract

Wetlands play an important role in the global carbon cycle as they can be sources or sinks for greenhouse gases. Groundwater discharge into wetlands can affect the water chemistry and act as a source of dissolved greenhouse gases, including CO_2 and CH_4. In this study, surface water quality parameters and CO_2 and CH_4 concentrations were evaluated in a tidal wetland (Hunter Wetlands National Park, Australia) using time series measurements. Radon (^{222}Rn), a natural groundwater tracer, was used to investigate the role of groundwater as a pathway for transporting dissolved CO_2 and CH_4 into the wetland. In addition, water-to-air CO_2 and CH_4 fluxes from the wetland were also estimated. The results showed a high concentration of radon in wetland surface water, indicating the occurrence of groundwater discharge. Radon concentration had a strong negative relationship with water depth with a determination coefficient (R^2) of 0.7, indicating that tidal pumping was the main driver of groundwater discharge to the wetland. Radon concentration also showed a positive relationship with CO_2 and CH_4 concentrations ($R^2 = 0.4$ and 0.5, respectively), while the time series data revealed that radon, CO_2, and CH_4 concentrations peaked concurrently during low tides. This implied that groundwater discharge was a source of CO_2 and CH_4 to the wetland. The wetland had an average water-to-air CO_2 flux of 99.1 mmol/($m^2 \cdot d$), twice higher than the global average CO_2 flux from wetlands. The average CH_4 flux from the wetland was estimated to be 0.3 mmol/($m^2 \cdot d$), which is at the higher end of the global CH_4 flux range for wetlands. The results showed that groundwater discharge could be an important, yet unaccounted source of CO_2 and CH_4 to tidal wetlands. This work has implications for tidal wetland carbon budgets and emphasizes the role of groundwater as a subsurface pathway for carbon transport.

Keywords: Groundwater discharge; Methane; Carbon dioxide; Radon; Global warming; Climate change

1. Introduction

Coastal tidal wetlands contain a large amount of carbon in their sediments, as they can sequester atmospheric carbon dioxide (CO_2) up to five times faster than terrestrial ecosystems (Wang et al., 2019; Hinson et al., 2017). However, coastal wetlands can also add CO_2 and CH_4 to the atmosphere through sediments and water gas fluxes (Chmura et al., 2003; Rosentreter et al., 2018; Leopold et al., 2013). Most previous studies on coastal carbon budgets have focused on CO_2 fluxes from sediments to the atmosphere. However, hydrology can also play an important role in transporting dissolved carbon (Needelman et al., 2018; Davis et al., 2020; Atkins et al., 2017). Additionally, the water column in coastal wetlands can release large amounts of CO_2 and CH_4, counteracting its sediment burial (Macklin et al., 2014; Ruiz-Halpern et al., 2015; Kayranli et al., 2010). However, this component of the coastal carbon cycle is the least studied, and further investigation of the role played by hydrology and water movement in carbon cycling of coastal wetlands is required.

Coastal wetland hydrology consists of interconnected groundwater and surface water flows (Sadat-Noori et al., 2021b). Generally, the difference in pressure (hydraulic head) drives groundwater movement and can cause surface

* Corresponding author.
E-mail address: m.sadat-noori@unsw.edu.au (Mahmood Sadat-Noori).
Peer review under responsibility of Hohai University.

https://doi.org/10.1016/j.wse.2022.02.005

water to infiltrate pore spaces into sediments or cause groundwater to discharge to surface waters (Bizhanimanzar et al., 2019; Vidon et al., 2010; Porubsky et al., 2011). The interaction between groundwater and surface water allows and enhances geochemical reactions between terrestrial and aquatic systems because groundwater and surface water have different chemical compositions (May and Mazlan, 2014). Hence, groundwater discharge can regulate both surface water quality and quantity in coastal wetlands (Wang et al., 2018; Ganju et al., 2013; Sadat-Noori and Glamore, 2019).

CO_2 and CH_4 can be produced in the sediments of wetlands due to the mineralization of organic carbon by different microbes and plant-root respiration (Gudasz et al., 2010; Needelman et al., 2018). Due to the long residence time and the chemical interaction between water and sediment materials, groundwater tends to have higher concentrations of solutes, including CO_2, than surface water (Santos et al., 2009; Call et al., 2015). As such, even small amounts of groundwater discharge can transport dissolved carbon from the sediments to surface waters (Vidon et al., 2010; May and Mazlan, 2014). Once dissolved in groundwater, and as groundwater discharges from the sediment, CO_2 and CH_4 leave the sediment and can enter the atmosphere and contribute to global warming (Ferrón et al., 2007; Jurado et al., 2018). Groundwater exchange between sediment and surface water can be facilitated through tidal pumping in coastal wetlands (Gleeson et al., 2013; Call et al., 2015; Heron and Ridd, 2008). These processes are important to an ecosystem in terms of CO_2 and CH_4 emissions. Hence, groundwater−surface water interactions can substantially constrain coastal carbon budgets. However, this has been largely overlooked due to the difficulties of assessing groundwater discharge.

Radon (^{222}Rn) is a noble gas with conservative chemical behavior, and its concentration is several times higher in groundwater than in surface water (Burnett and Dimova, 2012; Atkins et al., 2013). Radon has a short half-life of 3.8 d, which is on the same time scale as many physical processes in coastal environments (Sadat-Noori et al., 2021a). This means that any presence of radon in surface water indicates recent (less than 3.8 d) groundwater discharge (Swarzenski, 2007; Davis et al., 2020). These properties make radon a useful groundwater tracer in surface water bodies, allowing for spatial and temporal assessment of the dynamics of groundwater and its interaction with surface water in coastal environments (Büyükuslu et al., 2018; Peterson et al., 2019; Burnett et al., 2010).

This study hypothesized that groundwater discharge drives water quality and CO_2 and CH_4 fluxes in tidal wetlands. This hypothesis was tested with field experiments. Time series data of water quality parameters (i.e., salinity, pH, and dissolved oxygen) were collected. Meanwhile, CO_2 and CH_4 concentrations were measured in the tidal wetland. Radon was used as a groundwater tracer to investigate the role of groundwater in driving surface water quality and CO_2 and CH_4 dynamics. In addition, water-to-air fluxes of CO_2 and CH_4 were calculated to assess whether the wetland was a source or a sink for greenhouse gases.

2. Materials and methods

2.1. Study site

Fieldwork was conducted on November 25−30, 2018 in a tidal wetland located in the Hunter Wetlands National Park, Newcastle, Australia (Fig. 1). The low-lying wetland has a small catchment of about 24×10^4 m^2 with an elevation up to 1.5 m (Australian Height Datum). The region is characterized by a temperate climate with an average annual precipitation of 1139 mm. Air temperature ranges from 17°C to 26°C in summer (December−February) and from 8°C to 18°C in winter (June−August). There is no upstream surface water flowing into this wetland, and the wetland water discharges into the Hunter River through an estuarine channel (with a width of 10 m and a length of 80 m) at the mouth of the wetland. The tidal wetland area is affected by semidiurnal tides with a tidal range of 1.5 m. The area received 25 mm of rainfall on the fourth day of sampling.

2.2. Water quality sampling

Physicochemical parameters of surface water were measured using a calibrated YSI EXO_2 water quality multiparameter sonde. Variables including pH (with an accuracy of ±0.1), salinity (with an accuracy of 0.1‰), dissolved oxygen (DO) concentration (with an accuracy of ±0.1 mg/L), temperature (with an accuracy of ±0.01°C), and water depth (with an accuracy of ±0.004 m) were collected at 15-min intervals. The concentration of fluorescent dissolved organic matter (fDOM) was also measured using the same sonde and used as a proxy for dissolved organic matter in the wetland water column. Wind speed data (with an accuracy of ±10%) were collected onsite using a weather station (Model PH1000). Current velocity and direction were measured in the channel using a Sontek Argonaut acoustic doppler current profiler at 15-min intervals.

A RAD7 radon-in-air detector was modified and used to measure the radon concentration in water. An ultraportable greenhouse gas analyzer (UGGA, Los Gatos Research) was

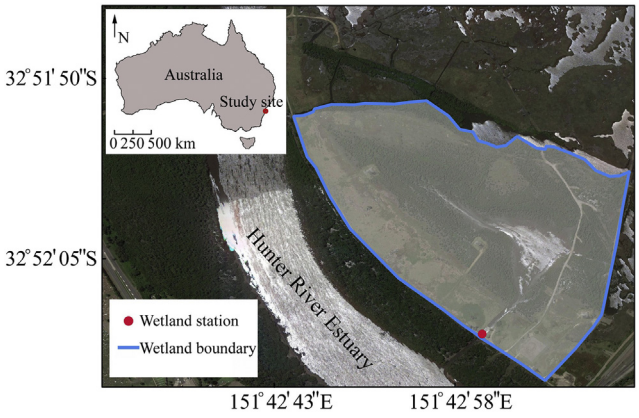

Fig. 1. Map of study site.

used to measure dissolved CO_2 and CH_4 in situ with data averaged over 1-min intervals and an uncertainty range less than 5%. To measure radon and greenhouse gases, these two systems were coupled, and surface water flow was continuously pumped at a rate of about 2.5 L/min from 30 cm below the surface into a shower-head gas equilibration device (GED) (Dulaiova et al., 2005). Dissolved gasses (e.g., radon) and air reached equilibrium in GED before the equilibrated air passed through RAD7 and UGGA. A pump was used to transfer the equilibrated air through drierite before it was returned to GED. In this setup, equilibrium times of around 5, 20, and 30 min were required for CO_2, CH_4, and radon, respectively (Webb et al., 2016; Santos et al., 2012b). Radon concentrations were measured every 30 min with uncertainties ranging from 10% at low tide to 60% at high tide. Radon solubility was calculated as a function of temperature and salinity (Schubert et al., 2012). Due to an unexpected technical issue with the UGGA device, some CO_2 and CH_4 data were lost on the fourth day of sampling.

2.3. Statistical analysis and flux calculations

Data were analyzed using the JASP (version 0.14.1) statistical software. Trends in the time series data were determined using the *Descriptive* model in JASP, and the Pearson correlation was used to examine the relationships between various parameters. According to the formula proposed by Wanninkhof (1992) based on gas transfer velocity and concentration gradient, the greenhouse gas fluxes for CO_2 and CH_4 (q) were estimated as follows:

$$q = k\alpha(C_{\text{water}} - C_{\text{air}}) \tag{1}$$

where k is the gas transfer velocity at the water−air interface, α is the solubility coefficient of the greenhouse gas, and C_{water} and C_{air} are the partial pressures of CO_2 and CH_4 in water and air, respectively. The solubility coefficients for CO_2 and CH_4 were estimated using the formulas proposed by Weiss (1974) and Wiesenburg and Guinasso (1979), respectively, as follows:

$$\ln \alpha_{CO_2} = -58.093 + \frac{90.506\,9 \times 100}{T} + 22.394 \ln\frac{T}{100} + S\left[0.027\,76 - \frac{0.025\,88T}{100} + 0.005\,057\left(\frac{T}{100}\right)^2\right] \tag{2}$$

$$\ln \alpha_{CH_4} = \ln f_G - 415.280 + \frac{596.810 \times 100}{T} + 379.259 \ln\frac{T}{100} - 62.075 \ln\frac{T}{100} + S\left[-0.059\,1 + \frac{0.032\,1T}{100} - 0.004\,81\left(\frac{T}{100}\right)^2\right] \tag{3}$$

where α_{CO_2} and α_{CH_4} are the solubility coefficients for CO_2 and CH_4, respectively; f_G is the molecular fraction in dry air for CH_4 (assumed to be constant at 1.41×10^{-6}); T is the temperature; and S is the salinity. The atmospheric partial pressure of CO_2 and CH_4 were assumed to be constant, with averaged values of 410×10^{-6} and 1.8×10^{-6} standard atmosphere pressure (atm), respectively. The gas transfer velocity (k) was estimated according to the five different empirical equations based on the common features in estuarine environments (e.g., wind speed, current velocity, and water depth) and Schmidt number of the gases (Table 1) (Borges et al., 2004; Ho et al., 2016; Jiang et al., 2008; Raymond and Cole, 2001; Sippo et al., 2017).

3. Results

3.1. Time series data of surface water

During sampling, the highest water depth was 1.7 m, and the lowest was 0.1 m (Fig. 2). Water salinity fluctuated between 33 and 36, indicating typical oceanic salinity values. However, salinity dropped to around 18 at the beginning of the fourth day of sampling due to the rainfall event. Temperature during sampling ranged from 17.2°C to 29.4°C, with an average temperature of 21.0°C. Temperature usually reached the peak values at about 16:00 to 20:00 and declined to the lowest values at about 6:00 to 9:00 (Fig. 2). pH ranged from 7.2 to 7.8, with a mean value of 7.6. Low pH values appeared during low tides. DO concentration was in a range from 46.5% to 110%, with an average value of 81.9%, and low DO concentration values occurred during low tides. The average water velocity and wind speed were 25.7 and 5.1 m/s, respectively. Radon concentrations ranged from 10 to 793 Bq/m^3, with an average value of 255 Bq/m^3 (Fig. 2). Radon concentrations followed an opposite trend to the tidal pattern and tended to increase during low tides and decrease during high tides.

Table 1
Gas transfer velocity and water-to-air fluxes of CO_2 and CH_4 estimated using various equations.

Equation	Average gas transfer velocity (m/d)	CO_2 flux (mmol/(m^2·d))	CH_4 flux (mmol/(m^2·d))	Reference
$k_{600} = 1 + 179W^{0.5}D^{-0.5} + 2.58U_{10}$	6.0	126.4	0.4	Borges et al. (2004)
$k_{600} = 0.77W^{0.5}D^{-0.5} + 0.026\,6U_{10}$	3.6	76.2	0.2	Ho et al. (2016)
$k_{600} = 0.314U_{10}^2 - 0.436U_{10} + 3.990$	3.4	71.7	0.2	Jiang et al. (2008)
$k_{600} = 1.91e^{0.35U_{10}}$	5.4	114.5	0.4	Raymond and Cole (2001)
$k_{600} = 1.58e^{0.3U_{10}} + 1.53W^{0.5}D^{-0.5}$	5.1	107.1	0.3	Sippo et al. (2017)
Average	4.7	99.1	0.3	

Note: k_{600} is the gas transfer velocity normalized to a Schmidt number value of 600 (m/d), W is the water velocity (cm/s), D is the water depth (m), and U_{10} is the wind speed at a height of 10 m (m/s).

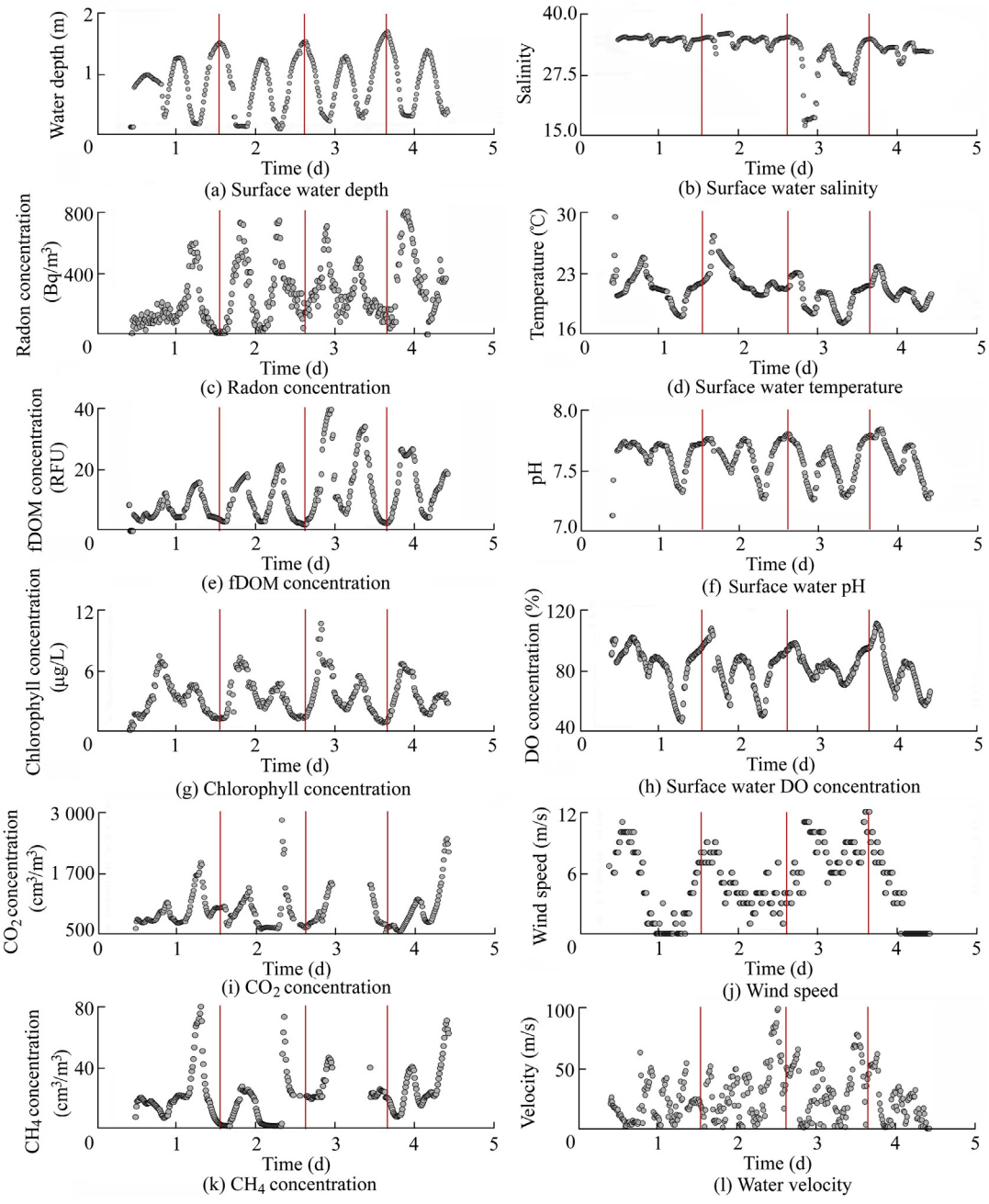

Fig. 2. Time series data of physical and chemical water quality parameters in wetland with red lines indicating daily highest high tides.

fDOM had a similar trend to radon and increased during low tides, with an average concentration of 10.6 relative fluorescence units (RFU). Chlorophyll had an average concentration of 3.4 μg/L and increased during low tides. CO_2 and CH_4 concentrations had similar trends to one another but followed opposite trends to the tidal pattern with increased concentrations during low tides. CO_2 and CH_4 concentrations ranged from 548.2 to 2 798.4 cm^3/m^3 and from 1.7 to 79.9 cm^3/m^3, with average concentrations of 980.2 and 21.6 cm^3/m^3, respectively.

Radon, chlorophyll, CH_4, and CO_2 concentrations all had weak negative correlations with salinity, with determination coefficient (R^2) values of 0.3, 0.4, 0.3, and 0.2, respectively. In contrast, radon, chlorophyll, and fDOM concentrations had strong negative correlations with water depth ($R^2 = 0.7$) while CO_2 and CH_4 concentrations had negative relationships with water depth ($R^2 = 0.5$) (Fig. 3). Radon concentration negatively correlated with pH ($R^2 = 0.6$) and DO concentration ($R^2 = 0.6$) and had strong positive correlations with chlorophyll ($R^2 = 0.6$) and fDOM concentrations ($R^2 = 0.7$). Radon

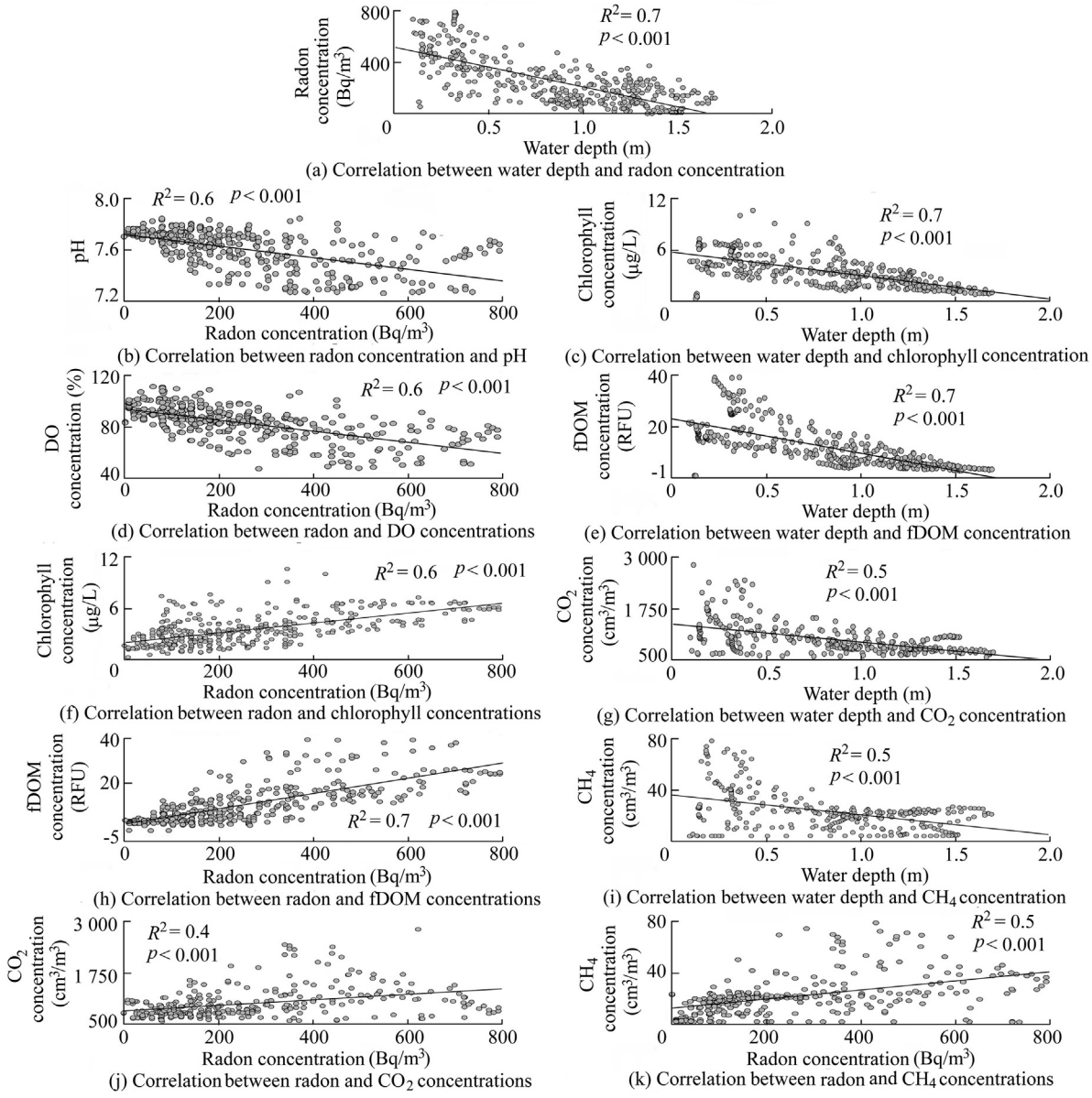

Fig. 3. Statistical correlation between water depth, radon, and water quality parameters.

concentration also had positive correlations with CO_2 ($R^2 = 0.4$) and CH_4 concentrations ($R^2 = 0.5$) (Fig. 3).

3.2. Wetland greenhouse gas fluxes to atmosphere

The average piston velocity obtained from the five empirical equations (Table 1) was calculated to be 4.7 m/s. The CO_2 flux ranged from 8.5 to 501.9 mmol/(m^2·d), with an average value of 99.1 mmol/(m^2·d). In contrast, the CH_4 flux had a range of 0−1.9 mmol/(m^2·d), with an average value of 0.3 mmol/(m^2·d). The CO_2 water-to-air flux was 330 times higher than the CH_4 flux (Table 1). The CO_2 and CH_4 fluxes from water to the atmosphere had similar trends across the five days of sampling and were strongly influenced by tides, with decreasing trends during high tides and peak values during low tides.

4. Discussion

4.1. Driving forces of groundwater discharge

High radon concentrations in surface water indicated the occurrence of groundwater discharge in the wetland. The observed negative correlation ($R^2 = 0.7$) between radon and water depth implied that tidal pumping was a driver of groundwater discharge in the wetland (Fig. 3). Tidal pumping occurs when estuary surface water infiltrates the permeable sediments and becomes groundwater during high tides. Afterwards, this water discharges from the sediment during low tides and returns to surface water due to gradient differences and hydrostatic pressure (Li et al., 2009; Li and Barry, 2000; Peterson et al., 2019). This recirculation of surface water can be important to the chemistry of water changes because

surface water interacts with sediment particles. Thus, the water that flows back to the surface water contains a new chemical signature (Taniguchi et al., 2019; Santos et al., 2012a; Burnett et al., 2006). Coastal wetlands with muddy environments may have low subsurface flow. However, the existence of numerous crab burrows creates preferential flow paths and contributes to the increase in the hydraulic conductivity (capability of enabling the movement of water) of the sediment, thereby increasing groundwater discharge (Gleeson et al., 2013; Heron and Ridd, 2008). The studied wetland contained many crab burrows, which facilitated local groundwater−surface water interactions.

4.2. Impact of groundwater discharge on surface water quality

DO in groundwater is consumed by organic decomposition of microorganisms in sediments and diffusion of reduced elements from the deeper layers of the sediment (Salles et al., 2006). The time series data (low DO during low tides) and the correlation between radon and DO concentrations ($R^2 = 0.6$) (Fig. 3) indicated that low oxygenated groundwater discharged into the wetland and reduced surface water DO during low tides. Groundwater with low DO can cause hypoxic conditions in surface water, reducing the overall water quality and damaging the ecosystem health (Davis et al., 2020; Carroll et al., 2021; Sammut et al., 1996). Several previous studies have reported that groundwater discharge delivering low DO water was the main source of hypoxia conditions in estuarine and coastal wetland environments (Guo et al., 2020; Peterson et al., 2016; McCoy et al., 2011). The time series data showed that surface water salinity decreased during low tides, but groundwater salinity was not sampled. It is speculated that the decrease in salinity was related to terrestrial groundwater inputs, as reported by other studies in which experiments were conducted in a similar environment (Tait et al., 2017).

Groundwater contains higher concentrations of chlorophyll and fDOM than surface water because microflora in sediments use abundant nutrients obtained from sediments to produce chlorophyll through primary production (Nelson et al., 1999; Null et al., 2012). The mineralization of organic matter in sediments is an important source of fDOM, which can be stored in groundwater in high amounts, especially in conditions in which oxygen is low (Burdige et al., 2004; Skoog et al., 1996). Here, the time series data indicated that the concentrations of chlorophyll and fDOM in the tidal wetland increased during low tides when groundwater discharge was the highest (Fig. 2). Furthermore, the strong positive relationships between radon concentration and both chlorophyll and fDOM concentrations (Fig. 3) indicated that groundwater discharge delivered chlorophyll and fDOM into the surface water. The high concentrations of chlorophyll and fDOM contribute to high light absorption and eutrophication, leading to increased amounts of algae and plankton and thereby causing anoxic events that further increase carbon fluxes (Nelson and Siegel, 2013; Valiela et al., 1990).

4.3. Groundwater discharge as a driving force for dissolved carbon in wetlands

Groundwater can contain high amounts of dissolved greenhouse gases. Thus, groundwater can be an important factor when determining whether wetlands act as a source of greenhouse gases to the atmosphere. Table 2 lists relevant studies on groundwater discharge as a source of greenhouse gases in coastal wetlands. Most previous studies have mainly been conducted in Australia and the United States and mostly in subtropical climate zones. There is a lack of data from the Middle East and South America and from temperate coastal

Table 2
Previous studies on groundwater discharge as a source of greenhouse gases in coastal ecosystems.

System	Location	Climate	Method	Reference
Wetland	McLeods Creek, New South Wales, Australia	Subtropical	Radon	Webb et al. (2016)
Estuary	North Creek, New South Wales, Australia	Subtropical	Radon	Maher et al. (2015)
Estuary	Hat Head, New South Wales, Australia	Subtropical	Radon	Sadat-Noori et al. (2016)
Embayment	Sydney Harbour, New South Wales, Australia	Subtropical	Radon	Reading et al. (2021)
Lake	Sydney, New South Wales, Australia	Temperate	Radon	Sadat-Noori et al. (2021c)
Mangrove creek	Kangaroo Island, Queensland, Australia	Subtropical	Radon	Call et al. (2015)
Natural and modified estuary	Gold Coast, Queensland, Australia	Subtropical	Radon	Macklin et al. (2014)
Natural and modified estuary	Bribie Island, Queensland, Australia	Subtropical	Radon	Davis et al. (2020)
Estuary	Brisbane, Queensland, Australia	Subtropical	Radon	Jeffrey et al. (2018)
Salt marsh wetland	Sapelo Island, Georgia, USA	Subtropical	Radium	Schutte et al. (2020)
Mangrove river estuary	Everglades National Park, USA	Subtropical	Radon	Reithmaier et al. (2020)
Coastal lake	Bethel, Alaska, USA	Subarctic	Radon	Dabrowski et al. (2020)
Estuary (wetland)	Squamish, British Columbia, Canada	Temperate	Radon	Diggle et al. (2019)
Central Amazon Basin	Rio Negro, Tapajós, Madeira, Brazil	Tropical	Radon	Call et al. (2018)
Tidal flats	Wadden Sea, Germany	Temperate	Radon	Santos et al. (2015)
Tidal basin	Georgetown County, USA	Subtropical	Radium	Cai et al. (2003)
Embayment	Chowder Bay, Australia	Temperate	Radon	Sadat-Noori et al. (2017)
Coral reef	Mabini, Batangas, the Philippines	Tropical	Radon	Correa et al. (2021)

wetlands. Groundwater rich in CO_2 and CH_4 was shown to be a major source of greenhouse gases in a subtropical estuary in Australia (Call et al., 2015), and Sadat-Noori et al. (2016) found that groundwater discharge was an important source of dissolved carbon and greenhouse gases in a subtropical wetland in Australia. This study filled a gap by reporting observations from a temperate coastal wetland.

Coastal wetlands can sequester large quantities of atmospheric carbon and store it in their sediments at a rate of 50% faster than terrestrial forests (Cui et al., 2018; Mcleod et al., 2011; Wang et al., 2019). Greenhouse gases such as CO_2 and CH_4 can be produced by the respiration of plant roots and microorganism activity in sediments as well as organic matter decomposition and mineralization (Gudasz et al., 2010; Needelman et al., 2018; Kaur et al., 2016). When in contact with groundwater, the sediment-based carbon dissolves in groundwater, enriching it with carbon. Hence, groundwater discharging to wetlands contains high concentrations of CO_2 and CH_4 even if in small quantities (Monger et al., 2015; Atkins et al., 2013; Akhand et al., 2016). Here, the time series data supported by the positive correlations of radon concentration with CO_2 and CH_4 concentrations indicated that groundwater was a source of CO_2 and CH_4 in the wetland (Figs. 2 and 4). Once in surface water, CO_2 and CH_4 can be exported to the open ocean or evade to the atmosphere, or both processes may take place (Santos et al., 2021).

4.4. Greenhouse gas fluxes to atmosphere from wetland surface water

The measurements showed that the wetland was supersaturated with CO_2 and CH_4. Hence, the wetland was a source of greenhouse gases in the atmosphere (Fig. 4). Carbon stored in the wetland's sediments and groundwater discharging into the wetland can provide CO_2 and CH_4 to the wetland surface water. In the study area, groundwater discharge could explain 40% of CO_2 variation and 50% of CH_4 variation in the wetland surface water. The concentrations of CO_2 and CH_4 gases reached their peaks during low tides in the wetland surface water, and the CO_2 and CH_4 peak fluxes also appeared at the same time due to these high concentrations (Fig. 4). Previous studies have also indicated that groundwater-derived carbon and greenhouse gases, especially CH_4 and nitrous oxide, can counteract carbon burial in coastal wetlands. However, this process is often overlooked in carbon budgets (Webb et al., 2016; Rosentreter et al., 2018).

Studies on greenhouse gas fluxes from coastal wetlands have mostly been conducted in tropical and subtropical areas, as presented in Table 3. Based on data from the literature, water-to-air CO_2 and CH_4 fluxes have been observed to decrease along with latitude and temperature, and tropical areas have been found to have higher fluxes than subtropical areas (Table 3). To put the observed estimates described herein in perspective, fluxes were compared with the global average available in the literature. The average CO_2 flux from the wetland was 99.1 mmol/(m^2·d) (Table 1), which is twice as high as the global average CO_2 emissions in lower estuaries

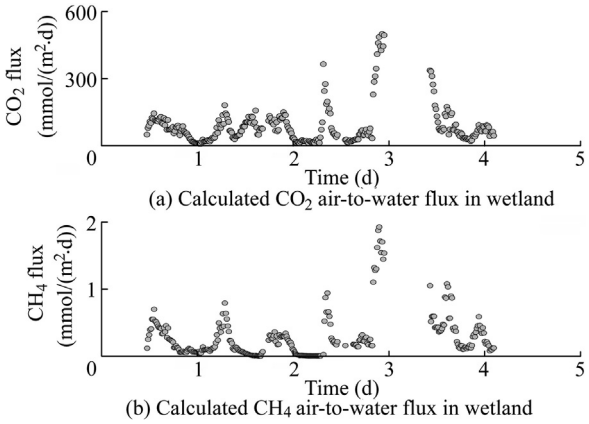

(a) Calculated CO_2 air-to-water flux in wetland

(b) Calculated CH_4 air-to-water flux in wetland

Fig. 4. Calculated CO_2 and CH_4 air-to-water fluxes in wetland.

(19.0−59.0 mmol/(m^2·d)) (Cai, 2011; Chen et al., 2013; Borges and Abril, 2011). The water-to-air flux also depends on the gas transfer velocity. In this study, this parameter was calculated using different methods to reduce the error associated with parameter estimation through empirical equations (Table 1).

The average CH_4 flux in the studied wetland was 0.3 mmol/(m^2·d) (Table 1), which is within the flux range from estuaries worldwide as reported in the literature (Table 3) and in the higher end of the range of global CH_4 fluxes in tidal estuaries (0.04−0.60 mmol/m^2/d) (Borges and Abril, 2011; Zhang et al., 2008; Ferrón et al., 2007). Water-to-air CH_4 fluxes can be controlled by tidal dynamics and reach their peak values during mid-to-low tides, when the strongest currents and the highest gas concentrations in the water column occur due to groundwater discharge (Rosentreter et al., 2018). In this study, the observed amount of CO_2 released into the atmosphere from the wetland was much larger than that of CH_4, indicating that CO_2 emissions dominated carbon gaseous fluxes. However, CH_4 is 34 times more potent as a greenhouse gas than CO_2, and even a small amount of CH_4 emission can have a greater impact on global warming than CO_2 (Cheng et al., 2021; Rosentreter et al., 2018). Hence, both CO_2 and CH_4 should be measured and considered when coastal wetland carbon budgets are developed.

5. Conclusions

Given that the relationship between coastal wetlands, groundwater, and greenhouse gases have not been widely understood, this study investigated greenhouse gas emissions from a tidal wetland and examined the role of groundwater discharge as a pathway for releasing greenhouse gases from wetland sediments. A 5-d radon time series dataset revealed strong groundwater−surface water interactions in the coastal wetland studied. The coupled measurements of radon, CO_2, and CH_4 at high temporal resolutions showed that groundwater discharge affected surface water chemistry. Radon concentration had a positive correlation with CO_2 and CH_4 concentrations. This indicated that groundwater discharge

Table 3
Previous studies on water-to-air greenhouse gas fluxes from coastal tidal wetland ecosystems.

System	Location	Latitude	Climate	CO_2 flux (mmol/(m^2·d))	CH_4 flux (μmol/(m^2·d))	Reference
Mangrove	Gazi Bay, Kenya	4°S	Tropical	115.9−192.8		Bouillon et al. (2007)
Estuaries	Brazil	4°S−5°S	Tropical	55 ± 45		Noriega and Araujo (2014)
Estuary	Nagada Creek, Papua New Guinea	5°S	Tropical	43.6 ± 33.2		Borges et al. (2003)
Mangrove creeks	Mtoni, Tanzania	6°S	Tropical	3.0−40.0	70.0−350.0	Kristensen et al. (2008)
Mangrove creeks	Ras Dege, Tanzania	6°S	Tropical	1.0−80.0	10.0−70.0	Kristensen et al. (2008)
Mangrove creek	Kiên Vàng, Viet Nam	8°N	Tropical	32.2 ± 39.4 (dry)		Koné and Borges (2008)
Mangrove creek	Kiên Vàng, Viet Nam	8°N	Tropical	154.7 ± 159.1 (wet)		Koné and Borges (2008)
Mangrove creek	Tam Giang, Viet Nam	8°N	Tropical	141.5 ± 117.8 (dry)		Koné and Borges (2008)
Mangrove creek	Tam Giang, Viet Nam	8°N	Tropical	128.5 ± 110.0 (wet)		Koné and Borges (2008)
Tidal mangrove creek	Wright Myo, India	11°N	Tropical		552.0−828.0	Barnes et al. (2006)
Estuary	Adyar, India	13°N	Tropical		3 600.0	Nirmal Rajkumar et al. (2008)
Lake estuary	South India	13°N	Tropical		54.0−280.0	Shalini et al. (2006)
Estuary	Gaderu Creek, India	17°N	Tropical	56.0 ± 100.9		Borges et al. (2003)
Rivers	Democratic Republic of the Congo	0°	Tropical	86.0−7 110.0	65.0−597 260.0	Borges et al. (2019)
Tidal mangrove creeks	Queensland, Australia	17°S−27°S	Subtropical	186.0 ± 19.2	4 800.0 ± 70.0	Rosentreter et al. (2017)
Tidal mangrove river	Florida, USA	25°N	Subtropical	217.7 ± 12.8		Rosentreter et al. (2017)
Tidal mangrove estuary	Florida, USA	25°N	Subtropical	171.0−232.0		Ho et al. (2014)
Estuary	Queensland, Australia	27°S	Subtropical	13.0−86.0		Macklin et al. (2014)
Estuary	North Creek, Australia	28°S	Subtropical	19.0−70.0	7.0−51.0	Maher et al. (2015)
Marsh-dominated estuary	Sapelo Island, Gabon	31°N	Subtropical	58.5−70.0		Wang and Cai (2004)
Estuary	Jiuduansha Island, China	31°N	Subtropical		30.0−400.0	Cheng et al. (2010)
Estuary	Yangtze, China	31°N	Subtropical		61.4 ± 22.6	Zhang et al. (2008)
Estuary	Coastal Georgia, USA	31°N	Subtropical	69.3		Jiang et al. (2008)
Mangrove bay	St. George's, Bermuda	32°N	Subtropical	59.8 ± 17.3		Zablocki et al. (2011)
Tidal mangrove creek	Kangaroo Island, Australia	35°S	Subtropical	201.56 ± 6.25	213.7 ± 10.6	Call et al. (2015)
Tidal estuaries	Bay of Cádiz, Spain	36°N	Temperate	73.0−177.0	34.0−150.0	Ferrón et al. (2007)
Estuaries	Europe	Above 39°N	Temperate	170.0		Frankignoulle et al. (1998)
Mud flats	Wadden Sea, Germany	53°N	Temperate	6.0−57.0		Santos et al. (2015)
Estuary	Newcastle, Australia	32°S	Subtropical	99.1	300.0	This study

could be a relevant pathway and a source of greenhouse gases to the wetland and contribute to the supersaturation of CO_2 and CH_4 in the wetland. The aquatic part of the wetland was found to be a source of greenhouse gases in the atmosphere with average water-to-air fluxes of 99.1 and 0.3 mmol/(m^2·d) for CO_2 and CH_4, respectively. The sampling supported the hypothesis that groundwater discharge can regulate surface water quality in a coastal wetland and be a driver of greenhouse gases in the wetland. Although this study did not quantify the groundwater discharge rate, it provides a basis for quantitative investigations of the role of groundwater as a source of greenhouse gases in coastal wetlands. Future carbon budgets should consider groundwater discharges when developing regional greenhouse gas budgets, and land managers should consider groundwater and surface water interactions when developing land management strategies.

Declaration of competing interest

The authors declare no conflicts of interest.

Acknowledgements

We would like to thank the University of New South Wales Sydney for supporting the fieldwork and data collection for this study. We also thank Hayley Ardagh from Newcastle Coal Infostructure Group (NCIG) for facilitating access to the site. We thank Christian Anibas for his help during fieldwork.

References

Akhand, A., Chanda, A., Manna, S., Das, S., Hazra, S., Roy, R., Choudhury, S.B., Rao, K.H., Dadhwal, V.K., Chakraborty, K., et al., 2016. A comparison of CO_2 dynamics and air−water fluxes in a river-dominated estuary and a mangrove-dominated marine estuary. Geophys. Res. Lett. 43(22), 11726−11735. https://doi.org/10.1002/2016GL070716.

Atkins, M.L., Santos, I.R., Ruiz-Halpern, S., Maher, D.T., 2013. Carbon dioxide dynamics driven by groundwater discharge in a coastal floodplain creek. J. Hydrol. 493, 30−42. https://doi.org/10.1016/j.jhydrol.2013.04.008.

Atkins, M.L., Santos, I.R., Maher, D.T., 2017. Seasonal exports and drivers of dissolved inorganic and organic carbon, carbon dioxide, methane and $\delta^{13}C$ signatures in a subtropical river network. Sci. Total Environ. 575, 545−563. https://doi.org/10.1016/j.scitotenv.2016.09.020.

Barnes, J., Ramesh, R., Purvaja, R., Nirmal Rajkumar, A., Senthil Kumar, B., Krithika, K., Ravichandran, K., Uher, G., Upstill-Goddard, R., 2006. Tidal dynamics and rainfall control N_2O and CH_4 emissions from a pristine mangrove creek. Geophys. Res. Lett. 33(15), L15405. https://doi.org/10.1029/2006GL026829.

Bizhanimanzar, M., Leconte, R., Nuth, M., 2019. Modelling of shallow water table dynamics using conceptual and physically based integrated surface-water−groundwater hydrologic models. Hydrol. Earth Syst. Sci. 23(5), 2245−2260. https://doi.org/10.5194/hess-23-2245-2019.

Borges, A.V., Djenidi, S., Lacroix, G., Théate, J., Delille, B., Frankignoulle, M., 2003. Atmospheric CO_2 flux from mangrove surrounding waters. Geophys. Res. Lett. 30(11), 1558. https://doi.org/10.1029/2003GL017143.

Borges, A.V., Delille, B., Schiettecatte, L.S., Gazeau, F., Abril, G., Frankignoulle, M., 2004. Gas transfer velocities of CO_2 in three European estuaries (Randers Fjord, Scheldt, and Thames). Limnol. Oceanogr. 49(5), 1630−1641. https://doi.org/10.4319/lo.2004.49.5.1630.

Borges, A.V., Abril, G., 2011. 5.04 - carbon dioxide and methane dynamics in estuaries. In: Wolanski, E., McLusky, D. (Eds.), Treatise on Estuarine and Coastal Science. Academic Press, Waltham, pp. 119−161.

Borges, A.V., Darchambeau, F., Lambert, T., Morana, C., Allen, G.H., Tambwe, E., Toengaho Sembaito, A., Mambo, T., Nlandu Wabakhangazi, J., Descy, J.P., et al., 2019. Variations in dissolved greenhouse gases (CO_2, CH_4, N_2O) in the Congo River network overwhelmingly driven by fluvial-wetland connectivity. Biogeosciences 16(19), 3801−3834. https://doi.org/10.5194/bg-16-3801-2019.

Bouillon, S., Dehairs, F., Velimirov, B., Abril, G., Borges, A.V., 2007. Dynamics of organic and inorganic carbon across contiguous mangrove and seagrass systems (Gazi Bay, Kenya). J. Geophys. Res. 112, G02018. https://doi.org/10.1029/2006JG000325.

Burdige, D.J., Kline, S.W., Chen, W., 2004. Fluorescent dissolved organic matter in marine sediment pore waters. Mar. Chem. 89(1), 289−311. https://doi.org/10.1016/j.marchem.2004.02.015.

Burnett, W.C., Aggarwal, P.K., Aureli, A., Bokuniewicz, H., Cable, J.E., Charette, M.A., Kontar, E., Krupa, S., Kulkarni, K.M., Loveless, A., et al., 2006. Quantifying submarine groundwater discharge in the coastal zone via multiple methods. Sci. Total Environ. 367(2), 498−543. https://doi.org/10.1016/j.scitotenv.2006.05.009.

Burnett, W.C., Peterson, R.N., Santos, I.R., Hicks, R.W., 2010. Use of automated radon measurements for rapid assessment of groundwater flow into Florida streams. J. Hydrol. 380(3), 298−304. https://doi.org/10.1016/j.jhydrol.2009.11.005.

Burnett, W.C., Dimova, N., 2012. A radon-based mass balance model for assessing groundwater inflows to lakes. In: Taniguchi, M., Shiraiwa, T. (Eds.), The Dilemma of Boundaries: Toward a New Concept of Catchment. Springer, Tokyo, pp. 55−66.

Büyükuslu, H., Özdemir, F.B., Öge, T.Ö., Gökce, H., 2018. Indoor and tap water radon (^{222}Rn) concentration measurements at Giresun University campus areas. Appl. Radiat. Isot. 139, 285−291. https://doi.org/10.1016/j.apradiso.2018.05.027.

Cai, W.J., Wang, Y., Krest, J., Moore, W.S., 2003. The geochemistry of dissolved inorganic carbon in a surficial groundwater aquifer in North Inlet, South Carolina, and the carbon fluxes to the coastal ocean. Geochem. Cosmochim. Acta 67(4), 631−639. https://doi.org/10.1016/S0016-7037(02)01167-5.

Cai, W.J., 2011. Estuarine and coastal ocean carbon paradox: CO_2 sinks or sites of terrestrial carbon incineration? Ann. Rev. Mar. Sci. 3, 123−145. https://doi.org/10.1146/annurev-marine-120709-142723.

Call, M., Maher, D.T., Santos, I.R., Ruiz-Halpern, S., Mangion, P., Sanders, C.J., Erler, D.V., Oakes, J.M., Rosentreter, J., Murray, R., et al., 2015. Spatial and temporal variability of carbon dioxide and methane fluxes over semi-diurnal and spring−neap−spring timescales in a mangrove creek. Geochem. Cosmochim. Acta 150, 211−225. https://doi.org/10.1016/j.gca.2014.11.023.

Call, M., Sanders, C.J., Enrich-Prast, A., Sanders, L., Marotta, H., Santos, I.R., Maher, D.T., 2018. Radon-traced pore-water as a potential source of CO_2 and CH_4 to receding black and clear water environments in the Amazon Basin. Limnol. Oceanogr. Let. 3(5), 375−383. https://doi.org/10.1002/lol2.10089.

Carroll, J.M., Kelly, J.L., Treible, L.M., Bliss, T., 2021. Submarine groundwater discharge as a potential driver of eastern oyster, *Crassostrea virginica*, populations in Georgia. Mar. Environ. Res. 170, 105440. https://doi.org/10.1016/j.marenvres.2021.105440.

Chen, C.T.A., Huang, T.H., Chen, Y.C., Bai, Y., He, X., Kang, Y., 2013. Air−sea exchanges of CO_2 in the world's coastal seas. Biogeosciences 10(10), 6509−6544. https://doi.org/10.5194/bg-10-6509-2013.

Cheng, C., Sun, T., Li, H., He, Q., Pavlostathis, S.G., Zhang, J., 2021. New insights in correlating greenhouse gas emissions and microbial carbon and nitrogen transformations in wetland sediments based on genomic and functional analysis. J. Environ. Manag. 297, 113280. https://doi.org/10.1016/j.jenvman.2021.113280.

Cheng, X., Luo, Y., Xu, Q., Lin, G., Zhang, Q., Chen, J., Li, B., 2010. Seasonal variation in CH_4 emission and its ^{13}C-isotopic signature from *Spartina alterniflora* and *Scirpus mariqueter* soils in an estuarine wetland. Plant Soil 327(1), 85−94. https://doi.org/10.1007/s11104-009-0033-y.

Chmura, G.L., Anisfeld, S.C., Cahoon, D.R., Lynch, J.C., 2003. Global carbon sequestration in tidal, saline wetland soils. Global Biogeochem. Cycles 17(4), 1111. https://doi.org/10.1029/2002GB001917.

Correa, R.E., Cardenas, M.B., Rodolfo, R.S., Lapus, M.R., Davis, K.L., Giles, A.B., Fullon, J.C., Hajati, M.C., Moosdorf, N., Sanders, C.J., et al., 2021. Submarine groundwater discharge releases CO_2 to a coral reef. ACS ES&T Water 1(8), 1756−1764. https://doi.org/10.1021/acsestwater.1c00104.

Cui, X., Liang, J., Lu, W., Chen, H., Liu, F., Lin, G., Xu, F., Luo, Y., Lin, G., 2018. Stronger ecosystem carbon sequestration potential of mangrove wetlands with respect to terrestrial forests in subtropical China. Agric. For. Meteorol. 249, 71−80. https://doi.org/10.1016/j.agrformet.2017.11.019.

Dabrowski, J.S., Charette, M.A., Mann, P.J., Ludwig, S.M., Natali, S.M., Holmes, R.M., Schade, J.D., Powell, M., Henderson, P.B., 2020. Using radon to quantify groundwater discharge and methane fluxes to a shallow, tundra lake on the Yukon-Kuskokwim Delta, Alaska. Biogeochemistry 148(1), 69−89. https://doi.org/10.1007/s10533-020-00647-w.

Davis, K., Santos, I.R., Perkins, A.K., Webb, J.R., Gleeson, J., 2020. Altered groundwater discharge and associated carbon fluxes in a wetland-drained coastal canal. Estuar. Coast. Shelf Sci. 235, 106567. https://doi.org/10.1016/j.ecss.2019.106567.

Diggle, R.M., Tait, D.R., Maher, D.T., Huggins, X., Santos, I.R., 2019. The role of porewater exchange as a driver of CO_2 flux to the atmosphere in a temperate estuary (Squamish, Canada). Environ. Earth Sci. 78(11), 1−13. https://doi.org/10.1007/s12665-019-8291-3.

Dulaiova, H., Peterson, R., Burnett, W., Lane-Smith, D., 2005. A multi-detector continuous monitor for assessment of ^{222}Rn in the coastal ocean. J. Radioanal. Nucl. Chem. 263(2), 361−363. https://doi.org/10.1007/s10967-005-0595-y.

Ferrón, S., Ortega, T., Gómez-Parra, A., Forja, J.M., 2007. Seasonal study of dissolved CH_4, CO_2 and N_2O in a shallow tidal system of the bay of Cádiz (SW Spain). J. Mar. Syst. 66(1), 244−257. https://doi.org/10.1016/j.jmarsys.2006.03.021.

Frankignoulle, M., Abril, G., Borges, A., Bourge, I., Canon, C., Delille, B., Libert, E., Théate, J.M., 1998. Carbon dioxide emission from European estuaries. Science 282(5388), 434−436. https://doi.org/10.1126/science.282.5388.434.

Ganju, N.K., Nidzieko, N.J., Kirwan, M.L., 2013. Inferring tidal wetland stability from channel sediment fluxes: Observations and a conceptual model: Inferring stability from sediment fluxes. J. Geophys. Res. Ear. Sur. 118(4), 2045−2058. https://doi.org/10.1002/jgrf.20143.

Gleeson, J., Santos, I.R., Maher, D.T., Golsby-Smith, L., 2013. Groundwater−surface water exchange in a mangrove tidal creek: Evidence from natural geochemical tracers and implications for nutrient budgets. Mar. Chem. 156, 27−37. https://doi.org/10.1016/j.marchem.2013.02.001.

Gudasz, C., Bastviken, D., Steger, K., Premke, K., Sobek, S., Tranvik, L.J., 2010. Temperature-controlled organic carbon mineralization in lake sediments. Nature 466(7305), 478−481. https://doi.org/10.1038/nature09186.

Guo, X., Xu, B., Burnett, W.C., Wei, Q., Nan, H., Zhao, S., Charette, M.A., Lian, E., Chen, G., Yu, Z., 2020. Does submarine groundwater discharge contribute to summer hypoxia in the Changjiang (Yangtze) River Estuary? Sci. Total Environ. 719, 137450. https://doi.org/10.1016/j.scitotenv.2020.137450.

Heron, S.F., Ridd, P.V., 2008. The tidal flushing of multiple-loop animal burrows. Estuar. Coast. Shelf Sci. 78(1), 135−144. https://doi.org/10.1016/j.ecss.2007.11.018.

Hinson, A.L., Feagin, R.A., Eriksson, M., Najjar, R.G., Herrmann, M., Bianchi, T.S., Kemp, M., Hutchings, J.A., Crooks, S., Boutton, T., 2017. The spatial distribution of soil organic carbon in tidal wetland soils of the

continental United States. Global Change Biol. 23(12), 5468−5480. https://doi.org/10.1111/gcb.13811.

Ho, D.T., Ferrón, S., Engel, V.C., Larsen, L.G., Barr, J.G., 2014. Air−water gas exchange and CO_2 flux in a mangrove-dominated estuary. Geophys. Res. Lett. 41(1), 108−113. https://doi.org/10.1002/2013GL058785.

Ho, D.T., Coffineau, N., Hickman, B., Chow, N., Koffman, T., Schlosser, P., 2016. Influence of current velocity and wind speed on air−water gas exchange in a mangrove estuary. Geophys. Res. Lett. 43(8), 3813−3821. https://doi.org/10.1002/2016GL068727.

Jeffrey, L.C., Santos, I.R., Tait, D.R., Makings, U., Maher, D.T., 2018. Seasonal drivers of carbon dioxide dynamics in a hydrologically modified subtropical tidal river and estuary (Caboolture River, Australia). J. Geophys. Res. Biogeosci. 123(6), 1827−1849. https://doi.org/10.1029/2017JG004023.

Jiang, L.Q., Cai, W.J., Wang, Y., 2008. A comparative study of carbon dioxide degassing in river- and marine-dominated estuaries. Limnol. Oceanogr. 53(6), 2603−2615. https://doi.org/10.4319/lo.2008.53.6.2603.

Jurado, A., Borges, A.V., Pujades, E., Briers, P., Nikolenko, O., Dassargues, A., Brouyère, S., 2018. Dynamics of greenhouse gases in the river−groundwater interface in a gaining river stretch (Triffoy catchment, Belgium). Hydrogeol. J. 26(8), 2739−2751. https://doi.org/10.1007/s10040-018-1834-y.

Kaur, S., Aggarwal, R., Lal, R., 2016. Assessment and mitigation of greenhouse gas emissions from groundwater irrigation. Irrigat. Drain. 65(5), 762−770. https://doi.org/10.1002/ird.2050.

Kayranli, B., Scholz, M., Mustafa, A., Hedmark, Å., 2010. Carbon storage and fluxes within freshwater wetlands: A critical review. Wetlands 30(1), 111−124. https://doi.org/10.1007/s13157-009-0003-4.

Koné, Y.J.M., Borges, A.V., 2008. Dissolved inorganic carbon dynamics in the waters surrounding forested mangroves of the Ca Mau Province (Vietnam). Estuar. Coast. Shelf Sci. 77(3), 409−421. https://doi.org/10.1016/j.ecss.2007.10.001.

Kristensen, E., Flindt, M.R., Ulomi, S., Borges, A.V., Abril, G.E., Bouillon, S., 2008. Emission of CO_2 and CH_4 to the atmosphere by sediments and open waters in two Tanzanian mangrove forests. Mar. Ecol. Prog. Ser. 370, 53−67. https://doi.org/10.3354/meps07642.

Leopold, A., Marchand, C., Deborde, J., Chaduteau, C., Allenbach, M., 2013. Influence of mangrove zonation on CO2 fluxes at the sediment−air interface (New Caledonia). Geoderma 62−70. https://doi.org/10.1016/j.geoderma.2013.03.008.

Li, L., Barry, D.A., 2000. Wave-induced beach groundwater flow. Adv. Water Resour. 23(4), 325−337. https://doi.org/10.1016/S0309-1708(99)00032-9.

Li, X., Hu, B.X., Burnett, W.C., Santos, I.R., Chanton, J.P., 2009. Submarine ground water discharge driven by tidal pumping in a heterogeneous aquifer. Groundwater 47(4), 558−568. https://doi.org/10.1111/j.1745-6584.2009.00563.x.

Macklin, P.A., Maher, D.T., Santos, I.R., 2014. Estuarine canal estate waters: Hotspots of CO_2 outgassing driven by enhanced groundwater discharge? Mar. Chem. 167, 82−92. https://doi.org/10.1016/j.marchem.2014.08.002.

Maher, D.T., Cowley, K., Santos, I.R., Macklin, P., Eyre, B.D., 2015. Methane and carbon dioxide dynamics in a subtropical estuary over a diel cycle: Insights from automated in situ radioactive and stable isotope measurements. Mar. Chem. 168, 69−79. https://doi.org/10.1016/j.marchem.2014.10.017.

May, R., Mazlan, N.S.B., 2014. Numerical simulation of the effect of heavy groundwater abstraction on groundwater−surface water interaction in Langat Basin, Selangor, Malaysia. Environ. Earth Sci. 71(3), 1239−1248. https://doi.org/10.1007/s12665-013-2527-4.

McCoy, C., Viso, R., Peterson, R.N., Libes, S., Lewis, B., Ledoux, J., Voulgaris, G., Smith, E., Sanger, D., 2011. Radon as an indicator of limited cross-shelf mixing of submarine groundwater discharge along an open ocean beach in the South Atlantic Bight during observed hypoxia. Continent. Shelf Res. 31(12), 1306−1317. https://doi.org/10.1016/j.csr.2011.05.009.

Mcleod, E., Chmura, G.L., Bouillon, S., Salm, R., Björk, M., Duarte, C.M., Lovelock, C.E., Schlesinger, W.H., Silliman, B.R., 2011. A blueprint for blue carbon: Toward an improved understanding of the role of vegetated coastal habitats in sequestering CO_2. Front. Ecol. Environ. 9(10), 552−560. https://doi.org/10.1890/110004.

Monger, H.C., Kraimer, R.A., Khresat, S.E., Cole, D.R., Wang, X., Wang, J., 2015. Sequestration of inorganic carbon in soil and groundwater. Geology 43(5), 375−378. https://doi.org/10.1130/G36449.1.

Needelman, B.A., Emmer, I.M., Emmett-Mattox, S., Crooks, S., Megonigal, J.P., Myers, D., Oreska, M.P.J., McGlathery, K., 2018. The science and policy of the verified carbon standard methodology for tidal wetland and seagrass restoration. Estuar. Coast. 41(8), 2159−2171. https://doi.org/10.1007/s12237-018-0429-0.

Nelson, J.R., Eckman, J.E., Robertson, C.Y., Marinelli, R.L., Jahnke, R.A., 1999. Benthic microalgal biomass and irradiance at the sea floor on the continental shelf of the South Atlantic Bight: Spatial and temporal variability and storm effects. Continent. Shelf Res. 19(4), 477−505. https://doi.org/10.1016/S0278-4343(98)00092-2.

Nelson, N.B., Siegel, D.A., 2013. The global distribution and dynamics of chromophoric dissolved organic matter. Ann. Rev. Mar. Sci. 5(1), 447−476. https://doi.org/10.1146/annurev-marine-120710-100751.

Nirmal Rajkumar, A., Barnes, J., Ramesh, R., Purvaja, R., Upstill-Goddard, R.C., 2008. Methane and nitrous oxide fluxes in the polluted Adyar River and Estuary, SE India. Mar. Pollut. Bull. 56(12), 2043−2051. https://doi.org/10.1016/j.marpolbul.2008.08.005.

Noriega, C., Araujo, M., 2014. Carbon dioxide emissions from estuaries of northern and northeastern Brazil. Sci. Rep. 4(1), 6164. https://doi.org/10.1038/srep06164.

Null, K.A., Dimova, N.T., Knee, K.L., Esser, B.K., Swarzenski, P.W., Singleton, M.J., Stacey, M., Paytan, A., 2012. Submarine groundwater discharge-derived nutrient loads to San Francisco Bay: Implications to future ecosystem changes. Estuar. Coast. 35(5), 1299−1315. https://doi.org/10.1007/s12237-012-9526-7.

Peterson, R.N., Moore, W.S., Chappel, S.L., Viso, R.F., Libes, S.M., Peterson, L.E., 2016. A new perspective on coastal hypoxia: The role of saline groundwater. Mar. Chem. 179, 1−11. https://doi.org/10.1016/j.marchem.2015.12.005.

Peterson, R.N., Meile, C., Peterson, L.E., Carter, M., Miklesh, D., 2019. Groundwater discharge dynamics into a salt marsh tidal river. Estuar. Coast. Shelf Sci. 218, 324−333. https://doi.org/10.1016/j.ecss.2019.01.007.

Porubsky, W.P., Joye, S.B., Moore, W.S., Tuncay, K., Meile, C., 2011. Field measurements and modeling of groundwater flow and biogeochemistry at Moses Hammock, a backbarrier island on the Georgia coast. Biogeochemistry 104(1), 69−90. https://doi.org/10.1007/s10533-010-9484-8.

Raymond, P.A., Cole, J.J., 2001. Gas exchange in rivers and estuaries: Choosing a gas transfer velocity. Estuaries 24(2), 312−317. https://doi.org/10.2307/1352954.

Reading, M., Tait, D., Maher, D., Jeffrey, L., Correa, R., Tucker, J., Shishaye, H., 2021. Submarine groundwater discharge drives nitrous oxide source/sink dynamics in a metropolitan estuary. Limnol. Oceanogr. 66, 1−22. https://doi.org/10.1002/lno.11710.

Reithmaier, G.M.S., Ho, D.T., Johnston, S.G., Maher, D.T., 2020. Mangroves as a source of greenhouse gases to the atmosphere and alkalinity and dissolved carbon to the coastal ocean: A case study from the everglades national Park, Florida. J. Geophys. Res. Biogeosci. 125(12), e2020JG005812. https://doi.org/10.1029/2020JG005812.

Rosentreter, J.A., Maher, D.T., Ho, D.T., Call, M., Barr, J.G., Eyre, B.D., 2017. Spatial and temporal variability of CO_2 and CH_4 gas transfer velocities and quantification of the CH_4 microbubble flux in mangrove dominated estuaries. Limnol. Oceanogr. 62(2), 561−578. https://doi.org/10.1126/sciadv.aao4985.

Rosentreter, J.A., Maher, D.T., Erler, D.V., Murray, R.H., Eyre, B.D., 2018. Methane emissions partially offset “blue carbon” burial in mangroves. Sci. Adv. 4(6), eaao4985. https://doi.org/10.1126/sciadv.aao4985.

Ruiz-Halpern, S., Maher, D.T., Santos, I.R., Eyre, B.D., 2015. High CO_2 evasion during floods in an Australian subtropical estuary downstream from a modified acidic floodplain wetland. Limnol. Oceanogr. 60(1), 42−56. https://doi.org/10.1002/lno.10004.

Sadat-Noori, M., Maher, D.T., Santos, I.R., 2016. Groundwater discharge as a source of dissolved carbon and greenhouse gases in a subtropical estuary. Estuar. Coast. 39(3), 639−656. https://doi.org/10.1007/s12237-015-0042-4.

Sadat-Noori, M., Tait, D.R., Maher, D.T., Holloway, C., Santos, I.R., 2017. Greenhouse gases and submarine groundwater discharge in a Sydney Harbour embayment (Australia). Estuar. Coast. Shelf Sci. 207, 499−509. https://doi.org/10.1016/j.ecss.2017.05.020.

Sadat-Noori, M., Glamore, W., 2019. Porewater exchange drives trace metal, dissolved organic carbon and total dissolved nitrogen export from a temperate mangrove wetland. J. Environ. Manag. 248, 109264. https://doi.org/10.1016/j.jenvman.2019.109264.

Sadat-Noori, M., Anibas, C., Andersen, M., Glamore, W., 2021a. A comparison of radon, heat tracer and head gradient methods to quantify surface water-groundwater exchange in a tidal wetland (Kooragang Island, Newcastle, Australia). J. Hydrol. 598, 126281. https://doi.org/10.1016/j.jhydrol.2021.126281.

Sadat-Noori, M., Rankin, C., Rayner, D., Heimhuber, V., Gaston, T., Drummond, C., Chalmers, A., Khojasteh, D., Glamore, W., 2021b. Coastal wetlands can be saved from sea level rise by recreating past tidal regimes. Sci. Rep. 11(1), 1−10. https://doi.org/10.1038/s41598-021-80977-3.

Sadat-Noori, M., Rutlidge, H., Andersen, M.S., Glamore, W., 2021c. Quantifying groundwater carbon dioxide and methane fluxes to an urban freshwater lake using radon measurements. Sci. Total Environ. 797, 149184. https://doi.org/10.1016/j.scitotenv.2021.149184.

Salles, P., Bredeweg, B., Araújo, S., 2006. Qualitative models about stream ecosystem recovery: Exploratory studies. Ecol. Model. 194(1), 80−89. https://doi.org/10.1016/j.ecolmodel.2005.10.018.

Sammut, J., White, I., Melville, M., 1996. Acidification of an estuarine tributary in eastern Australia due to drainage of acid sulfate soils. Mar. Freshw. Res. 47(5), 669−684. https://doi.org/10.1071/MF9960669.

Santos, I.R., Burnett, W.C., Dittmar, T., Suryaputra, I.G.N.A., Chanton, J., 2009. Tidal pumping drives nutrient and dissolved organic matter dynamics in a gulf of Mexico subterranean estuary. Geochem. Cosmochim. Acta 73(5), 1325−1339. https://doi.org/10.1016/j.gca.2008.11.029.

Santos, I.R., Eyre, B.D., Huettel, M., 2012a. The driving forces of porewater and groundwater flow in permeable coastal sediments: A review. Estuar. Coast. Shelf Sci. 98, 1−15. https://doi.org/10.1016/j.ecss.2011.10.024.

Santos, I.R., Maher, D.T., Eyre, B.D., 2012b. Coupling automated radon and carbon dioxide measurements in coastal waters. Environ. Sci. Technol. 46(14), 7685−7691. https://doi.org/10.1021/es301961b.

Santos, I.R., Beck, M., Brumsack, H.J., Maher, D.T., Dittmar, T., Waska, H., Schnetger, B., 2015. Porewater exchange as a driver of carbon dynamics across a terrestrial−marine transect: Insights from coupled ^{222}Rn and pCO_2 observations in the German Wadden Sea. Mar. Chem. 171, 10−20. https://doi.org/10.1016/j.marchem.2015.02.005.

Santos, I.R., Burdige, D.J., Jennerjahn, T.C., Bouillon, S., Cabral, A., Serrano, O., Wernberg, T., Filbee-Dexter, K., Guimond, J.A., Tamborski, J.J., 2021. The renaissance of Odum's outwelling hypothesis in 'Blue Carbon' science. Estuar. Coast. Shelf Sci. 255, 107361. https://doi.org/10.1016/j.ecss.2021.107361.

Schubert, M., Paschke, A., Lieberman, E., Burnett, W.C., 2012. Air−water partitioning of ^{222}Rn and its dependence on water temperature and salinity. Environ. Sci. Technol. 46(7), 3905−3911. https://doi.org/10.1021/es204680n.

Schutte, C.A., Moore, W.S., Wilson, A.M., Joye, S.B., 2020. Groundwater-driven methane export reduces salt marsh blue carbon potential. Global Biogeochem. Cycles 34(10), e2020GB006587. https://doi.org/10.1029/2020GB006587.

Shalini, A., Ramesh, R., Purvaja, R., Barnes, J., 2006. Spatial and temporal distribution of methane in an extensive shallow estuary, South India. J. Earth Syst. Sci. 115(4), 451−460. https://doi.org/10.1007/BF02702873.

Sippo, J.Z., Maher, D.T., Tait, D.R., Ruiz-Halpern, S., Sanders, C.J., Santos, I.R., 2017. Mangrove outwelling is a significant source of oceanic exchangeable organic carbon. Limnology and Oceanography Letters 2(1), 1−8. https://doi.org/10.1002/lol2.10031.

Skoog, A., Hall, P.O.J., Hulth, S., Paxéus, N., van der Loeff, M.R., Westerlund, S., 1996. Early diagenetic production and sediment−water exchange of fluorescent dissolved organic matter in the coastal environment. Geochem. Cosmochim. Acta 60(19), 3619−3629. https://doi.org/10.1016/0016-7037(96)83275-3.

Swarzenski, P.W., 2007. U/Th series radionuclides as coastal groundwater tracers. Chem. Rev. 107(2), 663−674. https://doi.org/10.1021/cr0503761.

Tait, D.R., Maher, D.T., Sanders, C.J., Santos, I.R., 2017. Radium-derived porewater exchange and dissolved N and P fluxes in mangroves. Geochem. Cosmochim. Acta 200, 295−309. https://doi.org/10.1016/j.gca.2016.12.024.

Taniguchi, M., Dulai, H., Burnett, K.M., Santos, I.R., Sugimoto, R., Stieglitz, T., Kim, G., Moosdorf, N., Burnett, W.C., 2019. Submarine groundwater discharge: Updates on its measurement techniques, geophysical drivers, magnitudes, and effects. Front. Environ. Sci. 7, 141. https://doi.org/10.3389/fenvs.2019.00141.

Valiela, I., Costa, J., Foreman, K., Teal, J.M., Howes, B., Aubrey, D., 1990. Transport of groundwater-borne nutrients from watersheds and their effects on coastal waters. Biogeochemistry 10(3), 177−197. https://doi.org/10.1007/BF00003143.

Vidon, P., Allan, C., Burns, D., Duval, T.P., Gurwick, N., Inamdar, S., Lowrance, R., Okay, J., Scott, D., Sebestyen, S., 2010. Hot spots and hot moments in riparian zones: Potential for improved water quality management. J. Am. Water Resour. Assoc. 46(2), 278−298. https://doi.org/10.1111/j.1752-1688.2010.00420.x.

Wang, F., Lu, X., Sanders, C.J., Tang, J., 2019. Tidal wetland resilience to sea level rise increases their carbon sequestration capacity in United States. Nat. Commun. 10(1), 5434. https://doi.org/10.1038/s41467-019-13294-z, 5411.

Wang, Y., Hu, Y., Yang, C., Chen, Y., 2018. Effects of vegetation types on water-extracted soil organic matter (WSOM) from riparian wetland and its impacts on riverine water quality: Implications for riparian wetland management. Sci. Total Environ. 628−629, 1249−1257. https://doi.org/10.1016/j.scitotenv.2018.02.061.

Wang, Z.A., Cai, W.J., 2004. Carbon dioxide degassing and inorganic carbon export from a marsh-dominated estuary (the Duplin River): A marsh CO_2 pump. Limnol. Oceanogr. 49(2), 341−354. https://doi.org/10.4319/lo.2004.49.2.0341.

Wanninkhof, R., 1992. Relationship between wind speed and gas exchange over the ocean. J. Geophys. Res. 97(C5), 7373−7382. https://doi.org/10.1029/92JC00188.

Webb, J.R., Santos, I.R., Tait, D.R., Sippo, J.Z., Macdonald, B.C.T., Robson, B., Maher, D.T., 2016. Divergent drivers of carbon dioxide and methane dynamics in an agricultural coastal floodplain: Post-flood hydrological and biological drivers. Chem. Geol. 440, 313−325. https://doi.org/10.1016/j.chemgeo.2016.07.025.

Weiss, R.F., 1974. Carbon dioxide in water and seawater: The solubility of a non-ideal gas. Mar. Chem. 2(3), 203−215. https://doi.org/10.1016/0304-4203(74)90015-2.

Wiesenburg, D.A., Guinasso, N.L., 1979. Equilibrium solubilities of methane, carbon monoxide, and hydrogen in water and sea water. J. Chem. Eng. Data 24(4), 356−360. https://doi.org/10.1021/je60083a006.

Zablocki, J.A., Andersson, A.J., Bates, N.R., 2011. Diel aquatic CO_2 system dynamics of a Bermudian mangrove environment. Aquat. Geochem. 17(6), 841−859. https://doi.org/10.1007/s10498-011-9142-3.

Zhang, G., Zhang, J., Liu, S., Ren, J., Xu, J., Zhang, F., 2008. Methane in the Changjiang (Yangtze River) Estuary and its adjacent marine area: Riverine input, sediment release and atmospheric fluxes. Biogeochemistry 91(1), 71−84. https://doi.org/10.1007/s10533-008-9259-7.